Radiolabeling of extracellular vesicles with ^{99m}Tc for quantitative *in vivo* imaging studies

Zoltán Varga[1], István Gyurkó[1], Krisztina Pálóczi[2], Edit I Buzás[2], Ildikó Horváth[3], Nikolett Hegedűs[3], Domokos Máthé[3,4], Krisztián Szigeti[3]

[1]Biological Nanochemistry Research Group, Institute of Materials and Environmental Chemistry, Research Centre for Natural Sciences, Hungarian Academy of Sciences, H-1117 Budapest, Hungary

[2]Department of Genetics, Cell- and Immunobiology and

[3]Department of Biophysics and Radiation Biology, Semmelweis University, H-1094 Budapest, Hungary

[4]CROmed Translational Research Centers, H-1047 Budapest, Hungary

Address correspondence to: Zoltán Varga; Biological Nanochemistry Research Group, Institute of Materials and Environmental Chemistry, Research Centre for Natural Sciences, Hungarian Academy of Sciences, Magyar tudósok körútja 2., H-1117, Budapest, Hungary, ű
E-mail: varga.zoltan@ttk.mta.hu

ABSTRACT

The biodistribution of extracellular vesicles (EVs) is a fundamental question in the field of circulating biomarkers, which has recently gained attention. Despite the capabilities of nuclear imaging methods such as single photon emission computed tomography (SPECT), radioisotope labeling of EVs and the use of the aforementioned methods for *in vivo* studies hardly can be found in the literature. In this paper we describe a novel method for the radioisotope labeling of erythrocyte-derived EVs using the ^{99m}Tc-tricarbonyl complex. Moreover, the capability of the developed labeling method for *in vivo* biodistribution studies is demonstrated in a mouse model. We found that the intravenously administered, ^{99m}Tc-labelled EVs mostly accumulated in the liver, and in the spleen. The *in vivo* stability of the labeled EVs was assessed by the comparison of the obtained biodistribution of EVs with that of the free ^{99m}Tc-tricarbonyl. According to our data, only a minor fraction of the radioactive label became detached from the EVs.

Key words

exosome, microvesicle, biodistribution, SPECT

Introduction

Extracellular vesicles (EVs) are recently recognized as key players in many physiological and pathological conditions.[1–6] EVs are not only present in all human body fluids, but also can be found for example in ocean water[7] and beer[8], due to the fact that yeasts and other microorganisms also release EVs. The clinical relevance of EVs was first recognized for their diagnostic use as biomarkers of different diseases[5]. Recently the therapeutic application of EVs is also emerging[9,10], for example, the application of dendritic cell (DC) derived exosomes for cancer treatment was recently under investigation in a clinical trial (NCT01159288). Understanding the role of these membrane vesicles in intercellular communication and also their applicability as vehicles for drug delivery requires the investigation of their biodistribution. The *in vivo* fate of EVs has only been addressed in the last few years, and most studies used fluorescent imaging for this purpose.[11–18] In these studies EVs were either labeled with a membrane dye[13,18] or engineered to display a membrane reporter (e.g. Gaussia luciferase), and administered exogenously[15] or utilized endogenously produced, genetically modified EVs (such as GFP-tagged CD63 bearing EVs)[19]. On the other hand, the application of nuclear imaging techniques such as single photon emission computed tomography (SPECT) or positron emission tomography (PET) utilizing isotopically labeled EVs hardly can be found in the literature, despite the fact that these techniques have indisputable advantages over fluorescent imaging regarding quantitative measurement of the biodistribution of the labeled compounds.[20] In this paper we report a novel method for radioisotope labeling of EVs using ^{99m}Tc-tricarbonyl complex, and demonstrate the applicability of this method for the non-invasive assessment of the biodistribution of erythrocyte-derived EVs using SPECT/CT.

Material and Methods

Preparation of erythrocyte vesicles

Erythrocyte vesicles were isolated from freshly outdated erythrocyte concentrates (Hungarian National Transfusion Service). The erythrocyte concentrate was two-fold diluted in phosphate buffered saline (PBS, Sigma-Aldrich, P4417), and the red blood cells were removed by two centrifugation steps at 1500 x g for 20 minutes at 4 C. EVs in the erythrocyte-free supernatant were concentrated by ultracentrifugation (Thermo Sorvall WX Ultracentrifuge, T-1270 fixed angle rotor) at 130 000 x g for 30 min and washed once with PBS using the same parameters. After re-suspending the EV pellet in PBS, the sample was

filtered through a 600 nm polycarbonate filter (Whatman® Nuclepore™), and finally snap frozen in 100 µl aliquots using liquid nitrogen and stored at -20 °C until use.

Freeze-Fracture Transmission Electron Microscopy (FF-TEM)

The vesicle sample (1-2 µl) was pipetted onto a gold sample holder, was frozen by plunging it immediately into partially solidified freon for 20 seconds and was stored in liquid nitrogen. Fracturing was performed at -100 °C in a Balzers freeze-fracture device (Balzers BAF 400D, Balzers AG, Vaduz, Liechtenstein). Replicas of the fractured faces etched at -100 °C were made by platinum-carbon shadowing and then cleaned with a water solution of surfactant and washed with distilled water. The replicas were placed on 200 mesh copper grids and examined in a MORGAGNI 268D (FEI, The Netherlands) transmission electron microscope.

Size Exclusion Chromatography combined with Dynamic Light Scattering (SEC-DLS)

SEC-DLS analysis was performed with a Jasco HPLC system (Jasco, Tokyo, Japan) consisting of a PU-2089 pump, an UV-2075 UV/Vis detector and a W130i online DLS detector (Avid Nano, High Wycombe, UK) controlled by the Chromnav software v. 1.17.02. Sepharose CL-2B gel was used as a stationary phase filled in a Tricorn 5/200 glass column (GE Healthcare Life Sciences). CL-2B is a cross-linked agarose gel with fractionation range of 70-40,000 kDa for dextran, and was found to be suitable for purification of EV samples [21]. The eluent was PBS, and the elution speed was 0.25 mL/min. The scattering intensity at 90 degrees and the autocorrelation function accumulated for 3 seconds was measured with the DLS setup equipped with a 660 nm laser. The online DLS data were processed with the iSize 3.0 software (Avid Nano Ltd., High Wycombe, UK).

Purification and concentration of erythrocyte derived EVs

Prior to labeling of the erythrocyte-derived EVs obtained by differential centrifugation, the EV sample was purified using a 10 mL plastic gravity column filled with the same Sepharose CL-2B gel used for the SEC-DLS investigation. 0.5 mL EV sample was introduced onto the column and PBS was used as the eluent. The EV-containing fraction corresponding to the void volume of the column was collected (1 mL) and further concentrated to 0.6 mL by using Vivaspin 500 centrifugal filters with 100 kDa MWCO (Sartorius Stedim Biotech GmbH).

99mTc labeling of the purified erythrocyte derived EVs

Radiolabeling of the erythrocyte-derived EVs was performed with the ^{99m}Tc-tricarbonyl complex $[^{99m}Tc(CO)_3(H_2O)_3]^+$ using a commercial kit (Isolink®, Mallinckrodt Medical B.V.), according to the manufacturer's instructions. 1.2 GBq $[^{99m}TcO_4]^-$ was eluted in 1 mL saline and added to the kit, followed

by placing the vial into boiling water for 20 minutes. The basic solution was neutralized by the addition of approx. 200 µL 1 M HCl solution. 0.6 mL of the EV sample was added to 0.8 mL ^{99m}Tc-tricarbonyl complex solution (430 MBq) and incubated for 30 min at room temperature. Separation of the free ^{99m}Tc-tricarbonyl was performed using a desalting column (Zeba™ Spin Desalting Column, 0.5 mL) applying the manufacturer's instructions.

In vivo SPECT/CT imaging

In vivo imaging was carried out on male BALB/c mice (n=3, Charles River Hungary). The body mass of the experimental animals was 28 ± 5 g and they were 10-12 week old. Animal experiments were carried out at the Nanobiotechnology & In Vivo Imaging Center, Semmelweis University, with permission from the local institutional animal ethics committee no. XIV-I-001/29-7/2012 and in compliance with the relevant European Union and Hungarian regulations. Images were acquired with a NanoSPECT/CT Silver Upgrade (Mediso Ltd., Budapest, Hungary) sequential animal SPECT/CT imaging system. In the SPECT/CT experiment 15 ± 2 MBq of ^{99m}Tc-labelled erythrocyte EVs in 200 µl volume was injected into the tail vein of the mice. Control measurements (n=3) were performed by injecting ^{99m}Tc-tricarbonyl complex only. During the scans the animals were continuously anaesthetized using a mixture of 1-1.5% isoflurane and medical oxygen. Their body temperature was maintained at 37 °C throughout the scanning. The SPECT scans started 1 hour after the time of administration, and the acquisition lasted 45 minutes.

To prevent movements, the animals were immobilized in a MultiCellTM Imaging Chamber (Mediso Ltd., Budapest, Hungary), and positioned in the center of field of view (FOV). The reconstructed voxel size was 300 µm in 120 × 120 × 328 pixel matrix both in SPECT and CT modalities. The image acquisitions were started with CT imaging after intravenous injection of ^{99m}Tc-labeled EVs. The CT and subsequent SPECT imaging lasted 10.5 and 30 min, respectively. Reconstructed, reoriented and co-registered images were further analyzed with Fusion (Mediso Ltd., Budapest, Hungary) and VivoQuant (inviCRO LLC, US) dedicated image analysis software by placing appropriate Volume of Interests (VOI) on the organs. The VOI were delineated manually on each CT scans. Radioactivity concentrations in MBq/cm^3 were determined for each volume of interest and corrected for scattering and isotopic decay in the reconstruction algorithm. The uptake values were measured in the following organs: heart, lungs, kidneys, liver, spleen, and bladder.

Results and Discussion

Fig. 1A shows the TEM images of the platinum-carbon replicas of the freeze-fractured EV sample. Spherical vesicles within the size range of 80 nm to 300 nm can be observed on these pictures, clearly demonstrating the applicability of the used isolation protocol. SEC-DLS analysis was used to characterize

the purity of the EV sample as well as to determine the mean hydrodynamic diameter of the vesicles (Fig.1B). During the SEC analysis, the EVs were excluded from the pores of the used gel (Sepharose CL-2B), and consequently they are eluted at shorter elution times (at 4.6 min in our case). The on-line DLS detector enabled the characterization of the mean size of the vesicle fraction, which was found to be 188 ± 11 nm (standard deviation). Smaller objects such as lipoproteins and soluble plasma proteins enter the pores of the gel, which results in longer elution times (at 14.3 min in our case). Due to the smaller size of the plasma proteins, their contribution cannot be detected based on the light scattering signal, but the UV absorption clearly indicates their presence in the studied sample.

Contamination by plasma proteins in EV samples is common when using isolation by differential centrifugation only. Therefore our sample was further purified prior to the radioisotope labeling. The purification was performed using the same Sepharose CL-2B gel that was used for the SEC-DLS analysis, but in a preparative manner using a 10 mL plastic tube and a gravity separation protocol. It was recently shown by Böing et al. that the contamination from high density lipoprotein is less than 5% and from plasma proteins is less than 1% in the purified EV-fraction by using this protocol.[21] The latter also agrees with our previous experience using the Sepharose CL-2B gel.

To the best of our knowledge no literature data is available for the radioisotope labeling of EVs. On the other hand, several approaches exist for the labelling of liposomes, which can be treated as model systems of the EVs due to the fact that the phospholipid bilayer represents the basic structural building block for both. The most commonly used radionuclide for liposomes labeling is ^{99m}Tc. There are several (afterloading and surface) radiolabeling techniques of liposomes in the literature[22]. The afterloading labeling technique based on the application of lipid soluble chelating agents[23]. One of the most frequently applied lipophilic chelator molecules is HMPAO (hexamethylpropyleneamineoxime). It is able to carry ^{99m}Tc inside the preformed vesicle, where the lipophilic HMPAO is transformed into its hydrophilic form in the presence of glutathione and HMPAO is trapped[22,24–32]. Another afterloading method for labeling liposomes uses ^{99m}Tc-BMEDA. This lipophilic radionuclide complex has very good in vitro and in vivo stability[22]. The direct surface labeling with ^{99m}Tc-pertechnetate is an easy manner of liposome labeling but the radiochemical yield, the specific activity and the stability of the forming complex seems to be very low[33].

Radiolabeling of artificial exosome-mimetic nanovesicles (ENVs) prepared by extrusion of macrophage cells was recently reported using the ^{99m}Tc-HMPAO method which is an established technique in liposome research.[34] The *in vivo* biodistribution of ENVs used as model system for real EVs was investigated using SPECT/CT. Although this method can be used in principle to label real EVs, the low

labeling efficiency of the HMPAO method at low concentrations in the case of liposomes might hinder the successful labeling of EVs.

In our experiment the novel organometallic aquaion, ^{99m}Tc-tricarbonyl was used for the radioisotope labeling of the purified EVs. This technique combines the advantages of high specific activity and small size of the labeling compound.[35] Hence it retains the biological activity of the labeled object. The ^{99m}Tc-tricarbonyl has been used for the labeling of a wide range of biomolecules from small tracer molecules, peptides, and antibodies to liposomes containing a DTPA chelater.[33,36] The ^{99m}Tc-tricarbonyl binds to several amino acids such as histidine, methionine, and cysteine,[37] consequently it was assumed that this aquaion will inherently bind to the surface of EVs due to the presence of membrane proteins of the vesicles. After the labeling procedure, the unbound ^{99m}Tc-tricarbonyl was removed by using desalting columns. The used desalting column removes more than 98% of the free ^{99m}Tc-tricarbonyl according to our previous experience, which also agrees with the specification from the manufacturer. By measuring the activities of the elutes and the columns, a labeling efficiency of 38.8 ± 6.2% was obtained for the erythrocyte derived EVs, which is reasonable, especially if the generally low concentration of EVs is considered.

Fig 2. shows a typical SPECT/CT image with the biodistribution of the labeled erythrocyte-derived EVs. High accumulation of the injected EVs can be observed in the liver and the spleen in accordance with previous fluorescent imaging studies. The activity appearing in the bladder can be attributed to the free ^{99m}Tc-tricarbonyl as demonstrated by a control measurement with the labeling compound. The real advantage of modern nuclear imaging methods is that the distribution of the labeled objects can be quantified without the need for removing the specific organs. In order to determine the percentage of the radioactivity in the different organs, appropriate VOIs were used. Fig. 3 shows the distribution of the labeled EVs within the different organs as a percentage of the total injected radioactivity (Fig. 3A) and also as standardized uptake value, known as SUV (Fig. 3B). SUV is defined as the ratio of the tissue radioactivity concentration and the injected activity divided by the body weight (as often used in PET). A major advantage of preclinical SPECT imaging is its ability to produce quantitative results for biodistribution,[38] just like PET imaging. SUV takes into account the volume of the segmented organ and so highlights organs with higher tissue uptake values.

The distribution values for the labeling compound alone are also presented in Fig. 3. The distributions of the free ^{99m}Tc-tricarbonyl and that of the labeled EVs differ significantly, which is an evidence of the successful labeling. The radioactivity detected in the bladder (3% of the injected radioactivity), originates from the free ^{99m}Tc-tricarbonyl that corresponds to the radiochemical purity of the labeled EV sample (taking into account the approx. 40% labeling efficiency and the 98% efficiency of the desalting columns

used to remove the remaining free ^{99m}Tc-tricarbonyl after labeling), which also indicates a good *in vivo* stability of the labeling.

The main aim of the SPECT/CT investigation of the ^{99m}Tc labeled erythrocyte-derived EVs was to demonstrate the applicability of the developed labeling procedure for in vivo experiments and to assess the in vivo stability of the labeling. The deep analysis of the biodistribution of erythrocyte-derived EVs is out of the scope of this paper, however, it can be compared to recent studies using fluorescently labeled EVs[13] and using ^{99m}Tc-labeled exosome-mimetic nanovesicles (ENVs)[34]. Wiklander et al. used a lipophilic near-infrared fluorescent dye (DiR: 1,1-dioctadecyl-3,3,3,3-tetramethy-lindotricarbocyanine iodide) that only fluoresces intensely when inserted into a lipid-membrane, to assess the biodistribution of EVs isolated from different cell lines. The obtained distribution of HEK293T cell derived EVs agrees well with our observation, namely high uptake of the EVs in the liver (60-80% of the total fluorescence, depending on the dose and way of administration), and in the spleen (10-20% of the total fluorescence). Wiklander et al. also investigated EVs from different sources, such as C2C12 mouse muscle cell line, B16F10 melanoma cells and primary immature bone marrow-derived DCs. The liver uptake was the highest among the organs in all cases, but interestingly, they have found differences for the extent of liver accumulation being the highest for the C2C12 cell-derived EVs (71 ± 1.5%) and the lowest for DC-derived EVs (46 ± 0.9%). Confirmation of these observations using radiolabeled EVs and using SPECT/CT (which is superior to fluorescent imaging regarding quantitative analysis), would be an interesting application of the ^{99m}Tc-tricarbonyl EV labelling procedure presented in this study.

The biodistribution obtained by Hwang et al. for ^{99m}Tc-HMPAO labeled ENVs from murine macrophage Raw 264.7 cell line shows also great similarity with the results presented in this paper[34]. Hwang et al. prepared ENVs by extrusion of whole cells and subsequent purification by gradient ultracentrifugation. High concentration of ENVs can be achieved by this method compared to natural EVs, which enabled the ^{99m}Tc-HMPAO labelling. On the other hand, the authors also mention in their manuscript that labeling of natural EVs with the ^{99m}Tc-HMPAO method is challenging due to the low radiochemical yield of the method at low EV concentrations[34].

In summary, a novel method for the radioisotope labeling of erythrocyte-derived EVs using ^{99m}Tc-tricarbonyl complex is presented. Special attention was paid to the purity of the EV sample that was achieved by SEC purification. This procedure assured that only EVs were labeled, since the used radiolabel could have also bound to free serum proteins. Acceptable radiochemical yield was achieved by the use of the novel ^{99m}Tc-tricarbonyl complex, which has high affinity to biomolecules. The applicability of the presented radiochemical labeling procedure was demonstrated by *in vivo* SPECT/CT imaging experiments using a mouse model which also confirmed the *in vivo* stability of the labeling. The presented

method might pave the way for further studies addressing the *in vivo* fate of EVs using nuclear imaging methods.

Acknowledgement

Part of this work was funded by the OTKA 111958, COST BM1202 ME HAD and MEDINPROT grants.

Disclosure Statement

No conflicting financial interests exist.

References

(1) Lee, T. H., D'Asti, E., Magnus, N., Al-Nedawi, K., Meehan, B., and Rak, J. (2011) Microvesicles as mediators of intercellular communication in cancer—the emerging science of cellular "debris." *Semin. Immunopathol. 33*, 455–467.
(2) Simons, M., and Raposo, G. (2009) Exosomes – vesicular carriers for intercellular communication. *Curr. Opin. Cell Biol. 21*, 575–581.
(3) Mathivanan, S., Ji, H., and Simpson, R. J. (2010) Exosomes: extracellular organelles important in intercellular communication. *J. Proteomics 73*, 1907–1920.
(4) Yuana, Y., Sturk, A., and Nieuwland, R. (2012) Extracellular vesicles in physiological and pathological conditions. *Blood Rev. 27*, 31–39.
(5) van der Pol, E., Böing, A. N., Harrison, P., Sturk, A., and Nieuwland, R. (2012) Classification, functions, and clinical relevance of extracellular vesicles. *Pharmacol. Rev. 64*, 676–705.
(6) György, B., Szabó, T. G., Pásztói, M., Pál, Z., Misják, P., Aradi, B., László, V., Pállinger, É., Pap, E., and Kittel, Á. (2011) Membrane vesicles, current state-of-the-art: emerging role of extracellular vesicles. *Cell. Mol. Life Sci. 68*, 2667–2688.
(7) Biller, S. J., Schubotz, F., Roggensack, S. E., Thompson, A. W., Summons, R. E., and Chisholm, S. W. (2014) Bacterial vesicles in marine ecosystems. *Science 343*, 183–186.
(8) (2014) Abstracts from the Third International Meeting of ISEV 2014 Rotterdam, The Netherlands, April 30th – May 3rd, 2014. *J. Extracell. Vesicles 3*, 24214.
(9) Andaloussi, S. E., Mäger, I., Breakefield, X. O., and Wood, M. J. (2013) Extracellular vesicles: biology and emerging therapeutic opportunities. *Nat. Rev. Drug Discov. 12*, 347–357.
(10) Lener, T., Gioma, M., Aigner, L., Börger, V., Buzas, E., Camussi, G., Chaput, N., Chatterjee, D., Del Portillo, H. A., and O'Driscoll, L. (2015) Applying extracellular vesicles based therapeutics in clinical trials-an ISEV position paper. *J. Extracell. Vesicles 4*.
(11) Zomer, A., Maynard, C., Verweij, F. J., Kamermans, A., Schäfer, R., Beerling, E., Schiffelers, R. M., de Wit, E., Berenguer, J., and Ellenbroek, S. I. J. (2015) In Vivo Imaging Reveals Extracellular Vesicle-Mediated Phenocopying of Metastatic Behavior. *Cell 161*, 1046–1057.
(12) Sadovska, L., Santos, C. B., Kalniņa, Z., and Linē, A. (2015) Biodistribution, Uptake and Effects Caused by Cancer-derived Extracellular Vesicles.
(13) Wiklander, O. P., Nordin, J. Z., O'Loughlin, A., Gustafsson, Y., Corso, G., Mäger, I., Vader, P., Lee, Y., Sork, H., and Seow, Y. (2015) Extracellular vesicle in vivo biodistribution is determined by cell source, route of administration and targeting. *J. Extracell. Vesicles 4*, 26316.
(14) Takahashi, Y., Nishikawa, M., Shinotsuka, H., Matsui, Y., Ohara, S., Imai, T., and Takakura, Y. (2013) Visualization and in vivo tracking of the exosomes of murine melanoma B16-BL6 cells in mice after intravenous injection. *J. Biotechnol. 165*, 77–84.
(15) Lai, C. P., Mardini, O., Ericsson, M., Prabhakar, S., Maguire, C. A., Chen, J. W., Tannous, B. A., and Breakefield, X. O. (2014) Dynamic biodistribution of extracellular vesicles in vivo using a multimodal imaging reporter. *ACS Nano 8*, 483–494.
(16) Jang, S. C., Kim, S. R., Yoon, Y. J., Park, K.-S., Kim, J. H., Lee, J., Kim, O. Y., Choi, E.-J., Kim, D.-K., and Choi, D.-S. (2015) In vivo Kinetic Biodistribution of Nano-Sized Outer Membrane Vesicles Derived from Bacteria. *Small 11*, 456–461.
(17) Grange, C., Tapparo, M., Bruno, S., Chatterjee, D., Quesenberry, P. J., Tetta, C., and Camussi, G. (2014) Biodistribution of mesenchymal stem cell-derived extracellular vesicles in a model of acute kidney injury monitored by optical imaging. *Int. J. Mol. Med. 33*, 1055–1063.

(18) Ohno, S., Takanashi, M., Sudo, K., Ueda, S., Ishikawa, A., Matsuyama, N., Fujita, K., Mizutani, T., Ohgi, T., and Ochiya, T. (2013) Systemically injected exosomes targeted to EGFR deliver antitumor microRNA to breast cancer cells. *Mol. Ther. 21*, 185–191.
(19) Suetsugu, A., Honma, K., Saji, S., Moriwaki, H., Ochiya, T., and Hoffman, R. M. (2013) Imaging exosome transfer from breast cancer cells to stroma at metastatic sites in orthotopic nude-mouse models. *Adv. Drug Deliv. Rev. 65*, 383–390.
(20) Hirsjärvi, S., Sancey, L., Dufort, S., Belloche, C., Vanpouille-Box, C., Garcion, E., Coll, J.-L., Hindré, F., and Benoit, J.-P. (2013) Effect of particle size on the biodistribution of lipid nanocapsules: Comparison between nuclear and fluorescence imaging and counting. *Int. J. Pharm. 453*, 594–600.
(21) Böing, A. N., Van Der Pol, E., Grootemaat, A. E., Coumans, F. A., Sturk, A., and Nieuwland, R. (2014) Single-step isolation of extracellular vesicles by size-exclusion chromatography. *J. Extracell. Vesicles 3*, 23430.
(22) Phillips, W. T., Goins, B. A., and Bao, A. (2009) Radioactive liposomes. *Wiley Interdiscip. Rev. Nanomed. Nanobiotechnol. 1*, 69–83.
(23) McAfee, J. G., and Thakur, M. L. (1976) Survey of radioactive agents for in vitro labeling of phagocytic leukocytes. I. Soluble agents. *J. Nucl. Med. Off. Publ. Soc. Nucl. Med. 17*, 480–487.
(24) Goins, B., Klipper, R., Rudolph, A. S., Cliff, R. O., Blumhardt, R., and Phillips, W. T. (1993) Biodistribution and imaging studies of technetium-99m-labeled liposomes in rats with focal infection. *J. Nucl. Med. Off. Publ. Soc. Nucl. Med. 34*, 2160–2168.
(25) Awasthi, V., Goins, B., McManus, L., Klipper, R., and Phillipsa, W. T. (2003) [99m Tc] liposomes for localizing experimental colitis in arabbit model. *Nucl. Med. Biol. 30*, 159–168.
(26) Lee, C.-M., Choi, Y., Huh, E. J., Lee, K. Y., Song, H.-C., Sun, M. J., Jeong, H.-J., Cho, C.-S., and Bom, H.-S. (2005) Polyethylene glycol (PEG) modified 99mTc-HMPAOliposome for improving blood circulation and biodistribution: the effect of the extent of PEGylation. *Cancer Biother. Radiopharm. 20*, 620–628.
(27) Dagar, S., Krishnadas, A., Rubinstein, I., Blend, M. J., and Önyüksel, H. (2003) VIP grafted sterically stabilized liposomes for targeted imaging of breast cancer: in vivo studies. *J. Controlled Release 91*, 123–133.
(28) Erdogan, S., Ozer, A. Y., Ercan, M. T., and Hincal, A. A. (2000) Scintigraphic imaging of infections with 99m-Tc-labelled glutathione liposomes. *J. Microencapsul. 17*, 459–465.
(29) Oyen, W. J., Boerman, O. C., Storm, G., Bloois, L. van, Koenders, E. B., Claessens, R. A., Perenboom, R. M., Crommelin, D. J., Meer, J. W. van der, and Corstens, F. H. (1996) Detecting infection and inflammation with technetium-99m-labeled Stealth (R) liposomes. *J. Nucl. Med. 37*, 1392–1396.
(30) Tilcock, C., Yap, M., Szucs, M., and Utkhede, D. (1994) PEG-coated lipid vesicles with encapsulated technetium-99m as blood pool agents for nuclear medicine. *Nucl. Med. Biol. 21*, 165–170.
(31) Sou, K., Goins, B., Takeoka, S., Tsuchida, E., and Phillips, W. T. (2007) Selective uptake of surface-modified phospholipid vesicles by bone marrow macrophages in vivo. *Biomaterials 28*, 2655–2666.
(32) Kleiter, M. M., Yu, D., Mohammadian, L. A., Niehaus, N., Spasojevic, I., Sanders, L., Viglianti, B. L., Yarmolenko, P. S., Hauck, M., and Petry, N. A. (2006) A Tracer Dose of Technetium-99m–Labeled Liposomes Can Estimate the Effect of Hyperthermia on Intratumoral Doxil Extravasation. *Clin. Cancer Res. 12*, 6800–6807.
(33) Helbok, A., Decristoforo, C., Dobrozemsky, G., Rangger, C., Diederen, E., Stark, B., Prassl, R., and von Guggenberg, E. (2010) Radiolabeling of lipid-based nanoparticles for diagnostics and therapeutic applications: a comparison using different radiometals. *J. Liposome Res. 20*, 219–227.
(34) Hwang, do W., Choi, H., Jang, S. C., Yoo, M. Y., Park, J. Y., Choi, N. E., Oh, H. J., Ha, S., Lee, Y. S., and Jeong, J. M. (2015) Noninvasive imaging of radiolabeled exosome-mimetic nanovesicle using (99m) Tc-HMPAO. *Sci. Rep. 5*, 15636.
(35) Alberto, R., Schibli, R., Egli, A., Schubiger, A. P., Abram, U., and Kaden, T. A. (1998) A novel organometallic aqua complex of technetium for the labeling of biomolecules: synthesis of [99mTc (OH2)

3 (CO) 3]+ from [99mTcO4]-in aqueous solution and its reaction with a bifunctional ligand. *J. Am. Chem. Soc. 120*, 7987–7988.
(36) Schibli, R., and Schubiger, A. P. (2002) Current use and future potential of organometallic radiopharmaceuticals. *Eur. J. Nucl. Med. Mol. Imaging 29*, 1529–1542.
(37) Egli, A., Alberto, R., Tannahill, L., and Schibli, R. (1999) Organometallic 99mTc-Aquaion labels peptide to an unprecedented high specific activity. *J. Nucl. Med. 40*, 1913.
(38) Veres, D. S., Máthé, D., Futó, I., Horváth, I., Balázs, Á., Karlinger, K., and Szigeti, K. (2014) Quantitative Liver Lesion Volume Determination by Nanoparticle-Based SPECT. *Mol. Imaging Biol. 16*, 167–172.

Figures

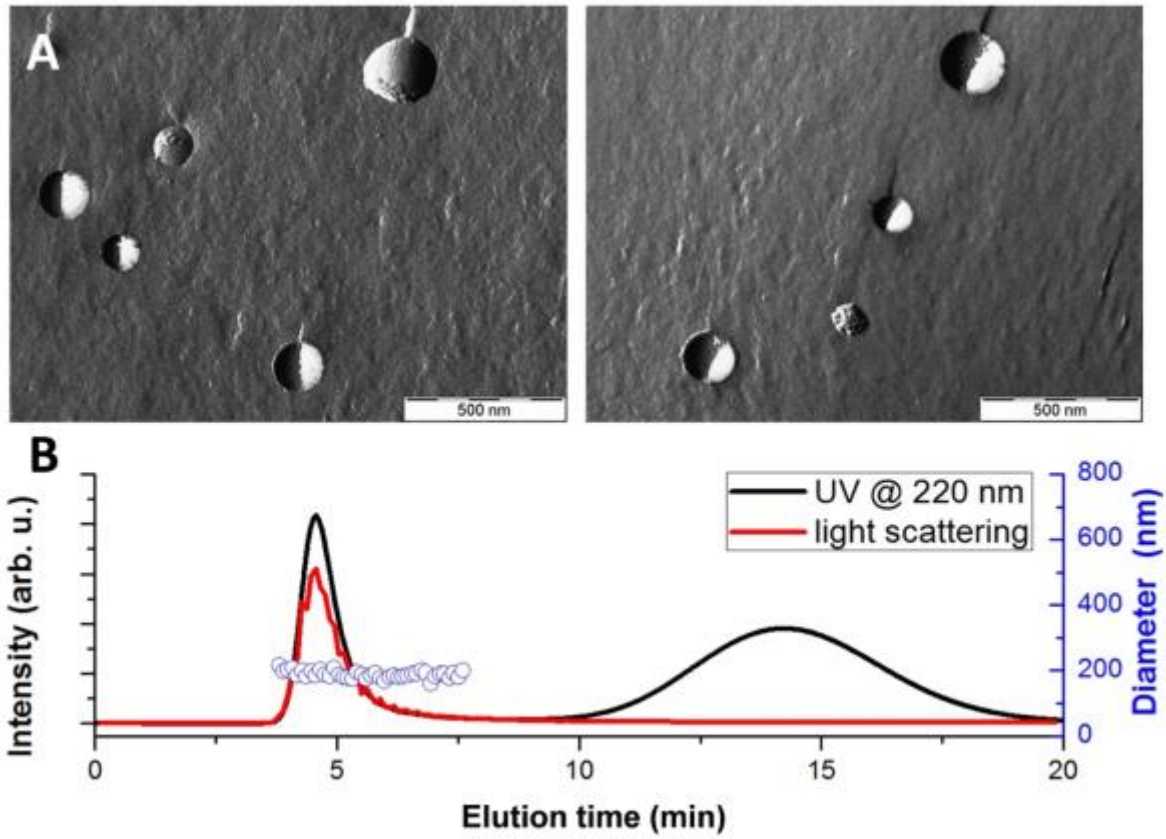

Fig. 1 (A) FF-TEM images of the erythrocyte-derived EVs. (B) SEC-DLS analysis of the erythrocyte-derived EVs using Sepharose CL-2B stationary phase. Black solid line represents the UV absorption signal while the red solid line corresponds to the static light scattering intensity at 90˚. Both signals indicate the EV fraction at 4.6 min elution time. The average size of the EVs was determined by the on-

line DLS data denoted by the symbols. The peak at 14.3 min corresponds to the protein contamination present in the sample, which is detectable only by the UV absorption signal.

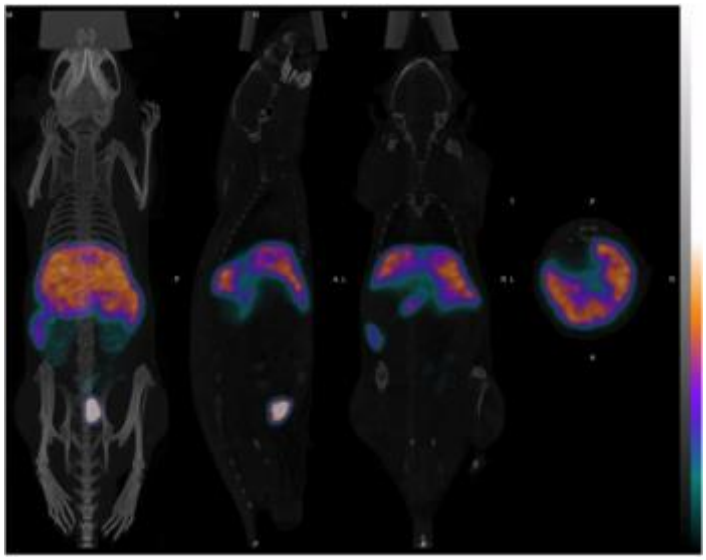

Fig. 2 In vivo SPECT-CT images of the ^{99m}Tc-labelled erythrocyte-derived EVs. The 3D reconstructed and co-registered SPECT and CT image is shown together with sagittal, coronal, and axial images (from left to right). Uptake of the EVs by the liver and spleen is clearly visible on the images, while the activity detected in the bladder corresponds to the ^{99m}Tc-tricarbonyl complex detached from the vesicles. (For color coded version of this figure, the reader is referred to the web version of the article.)

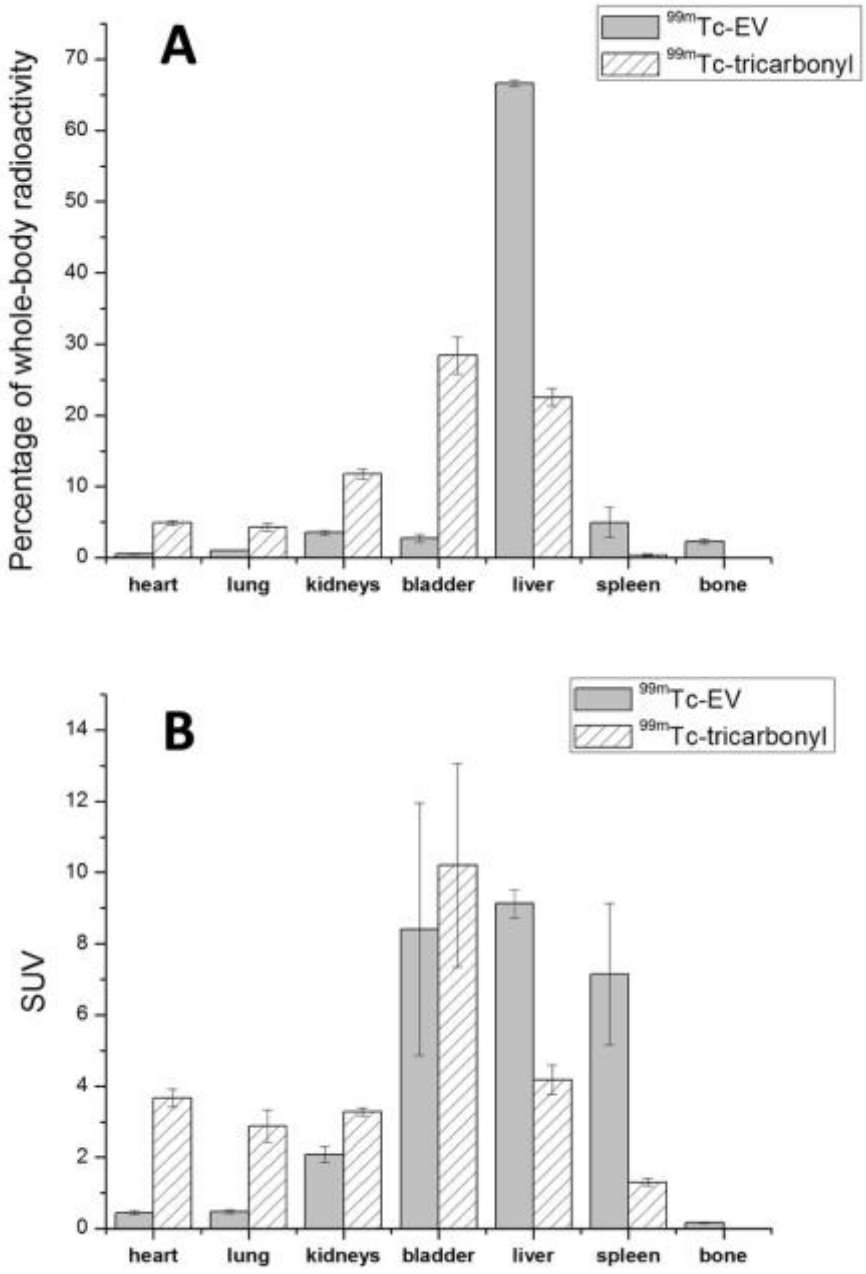

Fig. 3 Quantitative distribution of ^{99m}Tc-labelled erythrocyte-derived EVs together with the results of the control measurement performed by using the ^{99m}Tc-tricarbonyl complex alone. The activities measured in the specified organs in the percentage of the whole-body radioactivity are shown in A, and the standardized uptake values for the different organs are shown in B.